Transient behavior of superfluid turbulence in a large channel

K. W. Schwarz and J. R. Rozen
IBM Research Division, Thomas J. Watson Research Center, Yorktown Heights, New York 10598
(Received 25 March 1991)

The transient behavior of superfluid turbulence is studied theoretically and experimentally with the aim of understanding the disagreement between vortex-tangle theory and past measurements of free vortex-tangle decay in superfluid ^{4}He. Scaling theory is extended and large-scale simulations based on the reconnecting-vortex model are carried out. These imply that the Vinen equation should be a reasonable approximation even for rather large transients, and predict definite values for the Vinen parameters. Direct measurements of the vortex-tangle response to a sudden change in the driving velocity are seen to be in reasonable agreement with these predictions. It is found, however, that when the vortex tangle is allowed to decay farther toward zero, it eventually crosses over into a state of anomalously slow decay, which appears to be that observed in previous experiments. We argue that this regime should be interpreted in terms of a coupled-turbulence state in which random superfluid and normal-fluid motion interacts with the vortex tangle, the whole system decaying self-consistently at a rate controlled by the normal-fluid viscosity. Several additional qualitative observations which may be relevant to the question of how the vortex tangle is initiated are also reported.

I. INTRODUCTION

Superfluid ^{4}He at absolute zero acts like an irrotational, frictionless fluid, the motion of which can be characterized by a velocity field $\mathbf{v}_s$. At finite temperatures, the fluid also contains a gas of thermal excitations (the normal fluid) capable of moving with its own drift velocity $\mathbf{v}_n$ and having a temperature-dependent effective mass density ρ_n. Under various circumstances, when the relative velocity $\mathbf{v}_{ns}=\mathbf{v}_n-\mathbf{v}_s$ is made large enough, the superfluid enters a new dynamical state characterized by the appearance of a dense tangle of quantized vortex lines in the $\mathbf{v}_s$ field. This vortex-tangle state is driven and sustained by the frictional forces exerted by the normal fluid as it flows past the quantized vortices. A particularly easy way of generating a sizable v_{ns} in a channel is to seal off one end of the channel and place a heater there (Fig. 1). The normal fluid produced by the heater flows out of the channel with an average velocity $v_n=\dot{Q}/A\rho ST$, where $\dot{Q}$ is the heat input to the channel, A is the channel cross-sectional area, ρ is the total fluid density, S is the specific entropy, and T is the temperature. The normal fluid moving away from the heater is replaced by superfluid flowing in the opposite direction, the superfluid velocity being determined by the condition of zero net mass transport $\rho_n\mathbf{v}_n+\rho_s\mathbf{v}_s=0$. Since the normal and superfluid densities ρ_n and ρ_s are known functions of temperature, v_{ns} can then be varied in a controlled way simply by adjusting the heater input $\dot{Q}$.

Beginning with the seminal work of Vinen,[1] the properties of superfluid turbulence have been extensively investigated, mostly in capillaries of diameter 0.02 cm or less,[2] but also occasionally in large channels with cross-sectional dimensions on the order of a centimeter,[3,4] and in open geometries.[5] The properties of the steady, homogeneous, fully developed turbulent state observed in these experiments are now well understood on the basis of a fluid dynamical treatment of the quantized vortex tangle.[6] This approach is expected to provide a sound basis for the investigation of more complicated phenomena such as the onset of superfluid turbulence, the propagation of turbulent fronts, and the response of the vortex tangle to time-varying driving velocities.

The present paper reports a variety of observations on the transient behavior of superfluid turbulence in a large counterflow channel. The work was motivated by several unresolved questions concerning the time-dependent behavior of the vortex tangle. Of primary interest to us was the response of the fully developed, homogeneous state to sudden changes of the driving velocity v_{ns}. As we will show below, the theory of this state indicates that the well-known phenomenological equation of Vinen should provide a reasonable approximation to the resulting behavior, with the same scaling coefficients describing both growth and decay transients. In contradiction to this, the

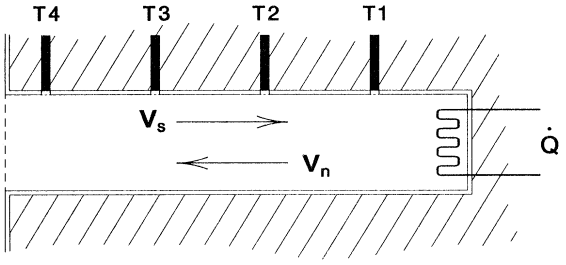

FIG. 1. Schematic rendering of the counterflow channel (not to scale). The details are discussed in the text.

early measurements of Vinen, as well as later measurements,[5] seem to show a very anomalous slow decay of the vortex line density when the driving velocity is suddenly reduced to zero. The question then is whether this disagreement indicates a serious flaw in the theory, or whether it implies that some interesting new physics is going on.

A secondary aim of the present experiment was to gain insight into how the turbulent state is initiated when the driving velocity is suddenly increased from zero. Previous large-channel experiments seem to show homogeneous growth of the vortex tangle along the entire channel. Indeed, in his initial work Vinen included a phenomenological vortex-growth term which he interprets as describing the nucleation of quantized vortex lines at the channel walls. This idea has no apparent basis in the context of the modern theory. Instead, our present physical picture suggests, roughly speaking, that the tangle can grow uniformly throughout the channel only if there exists a reasonably high, uniform density of quantized vortex lines to start with. If this is not the case, turbulence can only propagate in from vortex mills located at special points of the channel, such as the channel ends.[7] In support of this view, it has long been known[8,9] that in capillaries turbulence establishes itself by means of propagating fronts. It is of interest, therefore, to inquire why this phenomenon has not been observed in large channels, and why instead the turbulence appears to develop everywhere at once.

II. THEORETICAL CONSIDERATIONS

A. Dynamical scaling revisited

The theory of steady-state superfluid turbulence[6] can be extended to describe the response of the vortex tangle to a change in driving velocity. It will be assumed that the turbulence remains spatially homogeneous at all times, a condition which is likely to be a good approximation under many circumstances,[3,4] but which will clearly be inappropriate when, for example, there are propagating fronts. In contrast to the steady-state situation, the transient problem involves more than one important independent variable, and a generalization of the scaling arguments presented in Ref. 6 is needed. Representing the tangle by the curve $\mathbf{s}(\xi,t)$, where ξ is the arc length, the basic equation for vortex motion in the local approximation is[10]

$$\frac{\partial \mathbf{s}}{\partial t_0}=\mathbf{s}'\times\mathbf{s}''+\mathbf{v}_{s,0}+\alpha\mathbf{s}'\times(\mathbf{v}_{ns,0}-\mathbf{s}'\times\mathbf{s}'') -\alpha'\mathbf{s}'\times[\mathbf{s}'\times(\mathbf{v}_{ns,0}-\mathbf{s}'\times\mathbf{s}'')] \ . \tag{1}$$

Here t_0 is the reduced time βt, and $\mathbf{v}_{s,0}$, $\mathbf{v}_{ns,0}$ are the reduced velocities $\mathbf{v}_s/\beta$, $\mathbf{v}_{ns}/\beta$. The coefficient β is defined by

$$\beta=(\kappa/4\pi)\ln(c/\overline{|\mathbf{s}''|}a_0) \ , \tag{2}$$

where κ is the quantum of circulation, c is a constant of order one, $\overline{|\mathbf{s}''|}$ is the average curvature of the vortices in the tangle, and $a_0\simeq 1.3\times10^{-8}$ cm is the effective core radius of a quantized vortex. Although it can usually be treated as a constant, β has a logarithmic dependence on the tangle density since $\overline{|\mathbf{s}''|}$ increases as the tangle density increases. This can be important when comparing experiment and theory over a wide range of conditions. The primes in Eq. (1) denote derivatives with respect to the arc length, and α,α' are known temperature-dependent friction coefficients which characterize the effect of the normal fluid on the vortex motion. Equation (1) is supplemented by the condition that when a vortex approaches another vortex or a boundary sufficiently closely, a reconnection occurs.

Neglecting an unimportant logarithmic variation of the critical reconnection distance, this model has the feature that if one takes any solution of Eq. (1) and multiplies all distances by a scale factor λ, all velocities by λ^{-1}, and all times by λ^2, one obtains another solution of the equation. Any property $P(\mathbf{r},v_0,t_0,\ldots)$ evaluated on any particular solution of Eq. (1) will relate to P evaluated on the scaled solution according to

$$P(\lambda\mathbf{r},v_0/\lambda,t_0\lambda^2,\ldots)=f(\lambda)P(\mathbf{r},v_0,t_0,\ldots) \ , \tag{3}$$

where the form of $f(\lambda)$ depends on the particular combination of distances and times represented by P, and is usually obvious by inspection. To take a simple example, the evaluation of the line-length density at some point in the tangle involves measuring the length of quantized vortex line contained in some sampling volume and dividing by the sample volume. These scale as λ and λ^3, respectively, so that $f(\lambda)=\lambda^{-2}$ for the line-length density. Equation (3) can be written in the generic form

$$P(\lambda^{n_1}x_1,\ldots,\lambda^{n_k}x_k)=f(\lambda)P(x_1,\ldots,x_k) \ . \tag{4}$$

Suppose now that one knows the value of $P(x_1,\ldots,x_k)$ for only one particular value x_i^* of one particular variable, but all values of the remaining variables. Then one can find $P(x_1,\ldots,x_k)$ for other values $\lambda^{n_i}x_i^*$ of x_i by using the scaling condition

$$P(\lambda^{n_1}x_1,\ldots,\lambda^{n_i}x_i^*,\ldots,\lambda^{n_k}x_k) =f(\lambda)P(x_1,\ldots,x_i^*,\ldots,x_k) \ . \tag{5}$$

Renaming the variables $\lambda^{n_1}x_1\rightarrow x_1,\ldots,$ and using $\lambda^{n_i}x_i^*=x_i$ to define λ, one then finds

$$P(x_1,\ldots,x_k)=f(\lambda)P(x_1/\lambda^{n_1},\ldots,x_i^*,\ldots,x_k/\lambda^{n_k}) =f[x_i^{(1/n_i)}]g(x_1/x_i^{n_1/n_i},\ldots,x_k/x_i^{n_k/n_i}) \ . \tag{6}$$

Thus, the scaling symmetry allows one to write any property $P(x_1,\ldots,x_k)$ evaluated on a solution of Eq. (1) as a known function of any of the independent variables times a reduced function g of $k-1$ variables constructed as shown.

The relation (6) operates most potently when P depends on one variable only, since the variation can then be made to reside entirely in $f(\lambda)$. Such is the case for the steady-state, homogeneous vortex tangle discussed at

length in Ref. 6. To recall just one important example, suppose that the ensemble-averaged[11] line-length density $\bar{L}=\Omega^{-1}\int d\xi$ depends only on v_{ns}. Then $f(\lambda)=\lambda^{-2}$ and $n_1=-1$, and Eq. (6) implies a relation of the form

$$\bar{L}=c_L^2 v_{ns,0}^2=c_L^2(v_{ns}/\beta)^2 . \tag{7}$$

Numerous other examples relevant to the steady-state case are discussed in Ref. 6 and will be invoked here as needed.

B. Vinen's equation

The ensemble-averaged rate of change of line-length density was shown in Ref. 6 to be

$$\frac{d\bar{L}}{dt_0}=\frac{\alpha}{\Omega}\mathbf{v}_{ns,0}\cdot\int \mathbf{s}'\times\mathbf{s}''d\xi-\frac{\alpha}{\Omega}\int|\mathbf{s}'\times\mathbf{s}''|^2 d\xi , \tag{8}$$

and is thus seen to depend crucially on how the local self-induced vortex velocity $\mathbf{s}'\times\mathbf{s}''$ is distributed within the tangle. Suppose the tangle has achieved steady-state behavior. Then the ensemble-averaged integrals in Eq. (8) are functions of just one independent variable, most conveniently $\bar{L}$, and scaling gives

$$\Omega^{-1}\int \mathbf{s}'\times\mathbf{s}''d\xi=I_l\bar{L}^{3/2}\hat{\mathbf{v}}_{ns} , \tag{9}$$

$$\Omega^{-1}\int|\mathbf{s}'\times\mathbf{s}''|^2 d\xi=c_2^2\bar{L}^2 . \tag{10}$$

Inserting these relations into Eq. (8) leads to

$$\frac{d\bar{L}}{dt_0}=\alpha I_l v_{ns,0}\bar{L}^{3/2}-\alpha c_2^2\bar{L}^2 . \tag{11}$$

This has the form of the equation originally proposed by Vinen[1]

$$\frac{d\bar{L}}{dt}=\frac{\rho_n B}{2\rho}\chi_1 v_{ns}\bar{L}^{3/2}-\frac{\kappa}{2\pi}\chi_2\bar{L}^2 , \tag{12}$$

except that the Vinen coefficients χ_1 and χ_2 are now expressed in terms of quantities that have a clear microscopic interpretation and that can in fact be calculated from Eq. (1). One sees that the steady state is established by a competition between a growth term which depends on the self-induced velocity being distributed so as to point preferentially in the $\mathbf{v}_{ns}$ direction, and a decay term that depends only on how the magnitude of the self-induced velocity (i.e., the curvature) is distributed. From Eq. (7) one concludes that $c_L=I_l/c_2^2$, allowing the reexpression of c_2 or I_l in terms of c_L if so desired.

In the simplest instance we are interested in the situation where the vortex tangle is initially at some steady-state equilibrium $\bar{L}_i$ at a driving velocity $v_{ns,0}^i$, and the driving velocity is then suddenly changed to a different value $v_{ns,0}^f$ corresponding to a new equilibrium line length $\bar{L}_f=(I_l/c_2^2)^2(v_{ns,0}^f)^2$. It does not appear to be widely appreciated that Eq. (11) then has an analytical solution

$$\tau=-l^{-1/2}-\ln|1-l^{-1/2}|+\text{const} , \tag{13}$$

where $l=\bar{L}/\bar{L}_f$ and $\tau=\alpha c_2^2 t_0\bar{L}_f/2$. This solution, which embraces both growth and decay behavior, is graphed in Fig. 2. In truth, however, things are not quite as elementary as Eq. (13) suggests: although Vinen's equation was originally proposed as a phenomenological description of just this kind of transient behavior, there are in fact no theoretical arguments to support such an interpretation comparable to those which have been developed for the steady-state case. In particular, Eq. (11) as derived from the theory is a steady-state equation, and to apply it as a transient equation is to assume that at each instant in its evolution the vortex tangle adjusts itself so that $\mathbf{s}'\times\mathbf{s}''$ on average assumes the steady-state distribution appropriate to the instantaneous value of $\bar{L}(t)$. Clearly, there is no *a priori* reason to expect this to be true. The issue to be decided, therefore, is how good an approximation to the transient behavior Eq. (11) represents under various circumstances of interest.

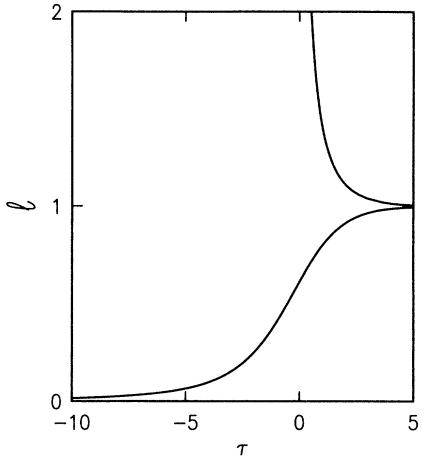

FIG. 2. Analytical solution of Vinen's equation when starting away from the steady state. The lower branch represents growth to the final steady state when $\bar{L}_i/\bar{L}_f<1$; the upper branch shows the decay when $\bar{L}_i/\bar{L}_f>1$. The time origin is fixed by the initial condition.

C. Beyond Vinen's equation

The variations in the internal structure of the vortex tangle when $\mathbf{v}_{ns}$ changes quickly and by a large amount cannot be addressed by scaling arguments alone, requiring instead a detailed dynamical study of how the tangle structure evolves. Such a study can be carried out by extending the numerical simulations of Ref. 6 to the transient case, the difference being that now we must calculate scaling functions g rather than just constants like c_L, I_l, and c_2 from the microscopic model. That is, the properties of the tangle now depend on the initial condition, the final condition, and the time; thus, the more general scaling analysis embodied in Eq. (6) comes into play in deciding what to calculate. It is convenient to choose t_0, $\bar{L}_i$, and $\bar{L}_f$ as the independent variables. It then follows from Eq. (6) that any property associated with the transient behavior can be written as $f(\bar{L}_f)g(t_0\bar{L}_f,\bar{L}_i/\bar{L}_f)$,

where f is known and g is a function that must be evaluated from the microscopic calculation.

The transient behavior is described by Eq. (8), not by Eq. (11). It is, however, still convenient to decompose the two integrals in Eq. (8) in a way which relates naturally to the steady-state theory. Accordingly, we assume that $\bar{L}(t_0)$ is still to be described by Eq. (11), which is equivalent to reinterpreting I_l and c_2^2 as time-dependent functions, now defined at each instant by Eqs. (9) and (10). These quantities must have their steady-state values at the beginning and end of the transient, and their deviation from these values during the transient provides a convenient measure of how much the vortex tangle deviates from the equilibrium distribution as it evolves. Since I_l and c_2^2 are dimensionless, they can be interpreted directly as g functions. Thus, we need to determine $\bar{L}(t_0)=\bar{L}_f g_L(t_0\bar{L}_f,\bar{L}_i/\bar{L}_f)$, $I_l(t_0\bar{L}_f,\bar{L}_i/\bar{L}_f)$, and $c_2^2(t_0\bar{L}_f,\bar{L}_i/\bar{L}_f)$. In addition, the actual experimental determination of the line-length density often proceeds indirectly through a measurement of the friction force exerted by the normal fluid as it flows past the vortex tangle:

$$\mathbf{F}_{sn}=-\frac{\rho_s\kappa\alpha\beta}{\Omega}\int \mathbf{s}'\times[\mathbf{s}'\times(\mathbf{v}_{ns,0}-\mathbf{s}'\times\mathbf{s}'')]d\xi\ . \quad (14)$$

The second part of the integral is easily seen to be proportional to (9), but the first part becomes

$$-\frac{\mathbf{v}_{ns,0}}{\Omega}\int[1-(\mathbf{s}'\cdot\hat{\mathbf{r}}_\parallel)^2]d\xi=-I_\parallel\bar{L}\mathbf{v}_{ns,0}\ , \quad (15)$$

where $\hat{\mathbf{r}}_\parallel$ is the unit vector in the direction of $\mathbf{v}_{ns}$. Equation (14) therefore involves a new structural scaling constant $I_\parallel$ representing a somewhat different aspect of the vortex-tangle geometry. Steady-state scaling then predicts[6]

$$\bar{F}_{sn}=\rho_s\kappa\alpha\beta[v_{ns,0}I_\parallel\bar{L}-I_l\bar{L}^{3/2}]\ , \quad (16a)$$

which , making the substitution (7), can also be written in the alternate forms

$$\bar{F}_{sn}=\rho_s\kappa\alpha(c_L^2I_\parallel-c_L^3I_l)v_{ns}^3/\beta^2 \quad (16b)$$

$$\bar{F}_{sn}=\rho_s\kappa\alpha(I_\parallel-c_LI_l)\bar{L}v_{ns}\ . \quad (16c)$$

If again we retain the form (16a) for the transient behavior, it also becomes of interest to determine $I_\parallel(t_0\bar{L}_f,\bar{L}_i/\bar{L}_f)$. At the beginning of the transient, $\bar{F}_{sn}$ changes discontinuously as $v_{ns,0}$ jumps from its initial to its final value. Remembering that $c_Lv_{ns,0}^f=\bar{L}_f^{1/2}$, the subsequent development is then described by the dimensionless function

$$\bar{F}_{sn}/\rho_s\kappa\alpha\beta\bar{L}^{3/2}=\frac{I_\parallel(t_0\bar{L}_f,\bar{L}_i/\bar{L}_f)}{c_L}g_L-I_l(t_0,\bar{L}_f,\bar{L}_i/\bar{L}_f)g_L^{3/2}\ . \quad (17)$$

To determine the g functions of interest completely is a large task for several reasons. First, the equations above are to be interpreted as averages over a suitable ensemble of individual vortex-tangle configurations. When applied to transients, we mean by this that one must compute the transient behavior for each member of a suitable ensemble of starting configurations, and then average the results together. Second, we are really interested in testing the accuracy of Vinen's equation for large transients, since it is obvious that it becomes exact in the limit of small changes in the driving velocity. Thus, we require calculations which go from very small to very large line-length densities. Third, in order to determine the g functions fully, the transients must be determined for the whole range of $\bar{L}_i/\bar{L}_f$. Finally, all of this should in prin-

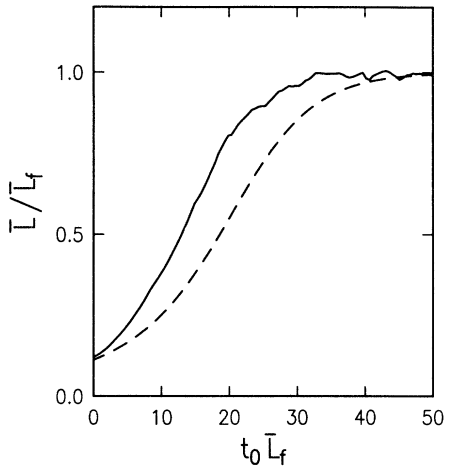

FIG. 3. Calculated growth of the line-length density when $v_{ns,0}$ is suddenly increased from 40 to 120. The dashed line is the prediction of Vinen's equation.

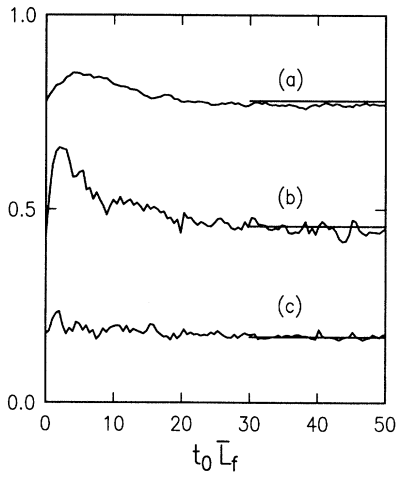

FIG. 4. Variation of the tangle-structure parameters during the growth transient of Fig. 3, showing (a) $I_\parallel$, (b) I_l, and (c) $c_2^2/20$. The horizontal lines are the steady-state values given in Ref. 6.

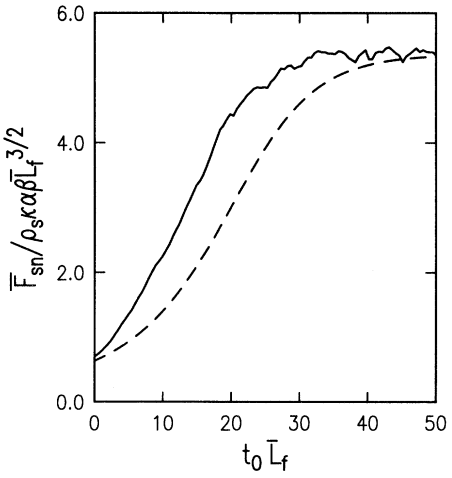

FIG. 5. Variation of the mutual friction force during the growth transient shown in Fig. 3. The dashed line is the behavior predicted assuming Vinen's equation and steady-state values for the structural parameters.

ciple be repeated for every temperature (i.e., α,α') of interest. The problem is not sufficiently interesting to warrant such a massive computational effort, and we have therefore focused on a more modest calculation aimed at getting a feeling for how good an approximation Eq. (11) is expected to be theoretically. To this end we have calculated transients for the largest and smallest value of $\bar{L}_f/\bar{L}_i$ that are computationally convenient, choosing just one representative temperature of 1.6 K ($\alpha=0.100$, $\alpha'=0.016$). The point, of course, is that values of $\bar{L}_f/\bar{L}_i$ closer to unity are certain to agree more closely with Eq. (11) than this worst case which we can investigate without too much difficulty.

The g functions $\bar{L}/\bar{L}_f$, I_l, c_2^2, $I_\parallel$, and $\bar{F}_{sn}/\rho_s\kappa\alpha\beta\bar{L}_f^{3/2}$ were computed for $\bar{L}_i/\bar{L}_f=1/9$ and for $\bar{L}_i/\bar{L}_f=9$ by switching $v_{sn,0}$ between the values of 40 and 120. The computational procedures have been described in Ref. 6. For each transient, five initial vortex-tangle configurations were randomly chosen from an appropriate steady-state run, and the individually calculated transients were then averaged together to obtain the results shown in the figures. The calculations (Figs. 3–8) show that, immediately after the driving velocity is changed, the integrals I_l and $I_\parallel$, which measure the directional anisotropy of the tangle structure, begin to deviate substantially from their steady-state values. The tangle becomes transiently more anisotropic if $v_{ns,0}$ is increased by a large amount (Fig. 4), and less so if $v_{ns,0}$ is decreased (Fig. 7), as might be expected since it is the driving velocity which forces the anisotropy to occur in the first place. On the other hand, the integral c_2^2 remains relatively undisturbed, implying that the kinkiness of the tangle depends primarily on the instantaneous value of $\bar{L}$, and is readjusted efficiently by the line-line reconnections as the line-length density evolves. When $v_{ns,0}$ is suddenly increased by a large amount, the growth behavior is dominated by the first term in Eqs. (8) or (11). Hence, the growth transients are seen in Figs. 3 and 5 to exhibit relatively large deviations from the quasiequilibrium theory. If $v_{ns,0}$ is decreased by a large amount, however, the second term in Eq. (8) or (11) dominates. The relatively weak variation in c_2^2 then implies that Vinen's equation should be more closely obeyed, as is indeed demonstrated in Figs. 6 and 8.

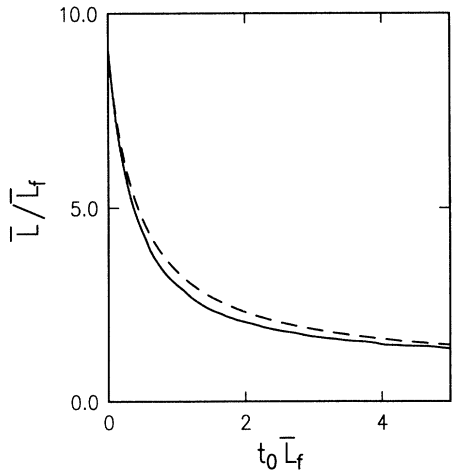

FIG. 6. Calculated decay of the line-length density when $v_{ns,0}$ is suddenly decreased from 120 to 40. The dashed line is the prediction of Vinen's equation.

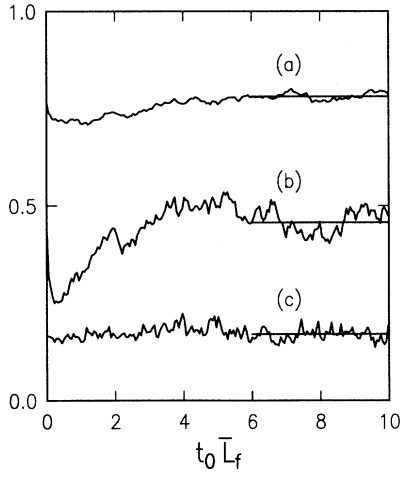

FIG. 7. Variation of the tangle-structure parameters during the decay transient of Fig. 6, showing (a) $I_\parallel$, (b) I_l, and (c) $c_2^2/20$. The horizontal lines are the steady-state values given in Ref. 6.

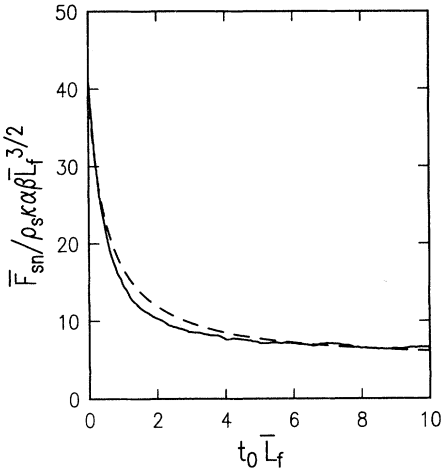

FIG. 8. Variation of the mutual friction force during the decay transient shown in Fig. 6. The dashed line is the behavior predicted assuming Vinen's equation and steady-state values for the structural parameters.

We conclude that it is possible to extend the reconnecting vortex-tangle model of Ref. 6 to determine the theoretical transient behavior of homogeneous superfluid turbulence. It is found that Vinen's equation provides a not unreasonable approximation to the computed transient behavior even for relatively large transients, with decay being modeled more accurately than growth. It is interesting for our purposes to ask how closely one can estimate the steady-state constants I_1 and c_2^2 by fitting Vinen's equation in the form of Eq. (11) to the observed transient behavior. Even for the large growth transient shown here, I_1 and c_2^2 as estimated in this way turn out to be accurate to within 25%. From a theoretical perspective, therefore, one expects to be able to obtain the steady-state coefficients I_1 and c_2^2 to within a few percent if one limits oneself to fitting transients much smaller than those studied here.

III. EXPERIMENTAL PROCEDURES

Our counterflow channel is immersed open-end down in a pumped helium bath approximately 30 L in volume. The temperature in the bath is measured and maintained by a Lake Shore DRC-82C temperature controller using a calibrated germanium resistor as a sensing element. With 60 mW applied to the bath-control heater, the bath temperature oscillates slowly and irregularity with an amplitude of 10 μK. Better short-term stability (2 μK) is achieved without the controller, but a slow steady drift of the bath temperature cannot then be avoided.

The counterflow channel (Fig. 1) consists of bronze waveguide tubing 1.00 by 2.32 cm in cross section and 24.0 cm in length, and is similar to that used in previous ion-trapping experiments. The driving heater at the top of the channel consists of a copper-gold alloy film about 800 Å thick, deposited on a sapphire substrate in a meander-line configuration to guarantee uniform heating. The heater presents a planar face to the channel and is connected in a four-wire configuration to allow an accurate measure of the power injected into the channel. Because of the large size of the channel, heater powers of hundreds of mW are required to generate the desired level of turbulence. In order to avoid the disruptive effects of switching such large heat loads on and off, the desired excitation power is switched between a compensating heater in the bath and the counterflow heater. This scheme allows the net power applied to the bath to remain constant. For certain measurements it was suspected that ambient vorticity in the bath was drifting into the channel and affecting the results. Some of the measurements were therefore done with a 100-lines-per-inch, 82% transmission, electroformed copper mesh placed across the open end of the channel.

The level of turbulence in the channel is determined in the conventional way by measuring the temperature gradient arising from the frictional force F_{sn} exerted by the normal fluid on the vortex tangle[1,2]

$$\nabla T = F_{sn}/\rho_s S \ , \tag{18}$$

where S is the entropy per unit mass. As is obvious from the previous discussion, measuring F_{sn} is not quite the same thing as measuring L directly, a comparison with theory requiring the inclusion of certain factors reflecting the anisotropic tangle geometry. To determine ∇T with some degree of spatial resolution, four matched, unencapsulated germanium resistance thermometers are mounted at intervals of 5.08 cm along the channel as indicated in Fig. 1. To ensure as ideal an interior channel surface as possible, each thermometer is recessed into a 0.38-cm-diam hole in the channel wall and the surface of the hole is covered with 40-lines-per-inch electroformed nickel screen.

The temperature difference between any two resistors is measured[4] by placing them into the arms of an ac bridge as shown in Fig. 9. Briefly, the ratio transformer

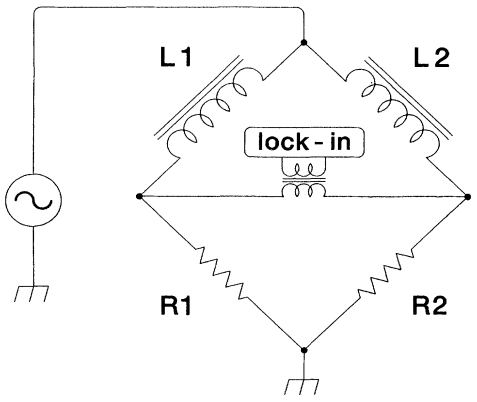

FIG. 9. Schematic rendering of the differential resistance measurement apparatus. This somewhat unconventional arrangement was found to give the best signal-to-noise ratio.

$L1$-$L2$ and a small trimming capacitor are adjusted to balance the bridge when there is no heat input to the channel and ∇T is zero. Power is then supplied to the channel heater to generate the vortex tangle, the resulting temperature changes δT_1 and δT_2 unbalancing the bridge as R_1 and R_2 change. It is easy to show that, to first order, the out-of-balance signal is given by

$$S = G\left[(\gamma_1-\gamma_2)\frac{\delta T_1+\delta T_2}{2} + \frac{\gamma_1+\gamma_2}{2}(\delta T_1-\delta T_2)\right]V , \quad (19)$$

where γ_i stands for $(dR_i/dT)/R_i$, V is the amplitude of the drive oscillator, and the coefficient G depends on the bridge parameters, on lock-in detector settings, and on many other factors. If the γ's are closely matched and the overall temperature rise is small, the observed signal will be directional proportional to the temperature difference ΔT that develops between the two resistors. In practice, the net sensitivity $G\gamma_i V$ of each individual thermometer is calibrated by first balancing the bridge at the working temperature, then replacing one of the resistors with an equivalent fixed dummy resistor, and then changing the bath temperature slightly to determine the response of the other resistor. A typical calibration allows us to determine the sensitivity to better than 0.5%. Since the net sensitivity depends on many factors, a new calibration is performed each time conditions are changed significantly. The variation in the sensitivity between individual thermometers, measured under identical conditions, is found to be about 2%, so that the common-mode error arising from overall temperature changes at the two resistors is reduced by a factor of about 50. The remaining common-mode error appears to be negligible in our experiments.

Since the measurements are done in a large channel at relatively high temperatures, and because thermometer self-heating effects are largely canceled by the differential nature of the measurement, it is possible to gain in sensitivity by applying quite high drive voltages (of order 0.15 V) to the bridge. With a lock-in response time of 10 ms, the typical fluctuations in the measured temperature are then of order 0.2 μK. In addition, the output of the lock-in detector is recorded by a signal-averaging digital oscilloscope interfaced to a computer. We find that, with a modest amount of signal averaging, a temperature sensitivity of order 0.02 μK can easily be achieved. A typical experimental signal is displayed in Fig. 10. Taken over the T_1 to T_4 distance, a sensitivity of 0.02 μK represents a temperature gradient of order 10^{-9} K cm^{-1}. While this appears quite sensitive, one can estimate from Eqs. (16c) and (18) that at 1.6 K it requires a line-length density of order 250 cm^{-2} to generate such a temperature gradient. This is still more than an order of magnitude above the critical line-length density characteristic of the turbulence onset.[12] Thus, the onset regime cannot be studied directly in our experiment, a characteristic disadvantage of large-channel experiments.

The idealized experimental goal is to change v_{ns} discontinuously, and to detect the temperature variations as they occur. It is found that both the heater and the thermometer respond on time scales short compared to the 5-ms minimum response time of the lock-in detector. Since this time is short compared to the measured transient times, the ideal experimental conditions are well enough approximated as regards signal detection. The generation of the discontinuous change in v_{ns} is less well realized because of Helmholtz oscillations which occur when the heater is switched.[1] The ringing can be largely eliminated by Vinen's trick of applying the heat pulse in two out-of-phase steps. However, this means that, in practice, it takes about 30 ms to effectuate a large change in the driving velocity.

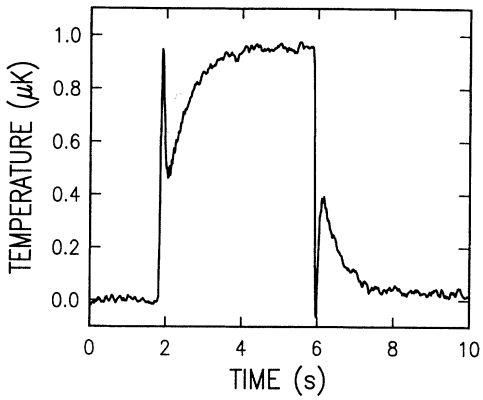

FIG. 10. Typical experimental signal, taken at $T=1.60$ K by stepping $\dot{Q}/A$ between 0.0427 and 0.0487 W cm^{-2}. The transient signal was acquired with a 30-ms time constant and averaged for 100 sweeps. The thermometer excitation was 0.1456 V rms, and the thermometer sensitivity 0.197 V/K.

IV. RESULTS

A. Steady-state measurements

Steady-state turbulence levels have been measured in many previous experiments[2] and, in general, accord well with the steady-state theory described in Ref. 6. There have, nevertheless, been some claims[13] that turbulence levels in large channels are in strong disagreement with the theory. Since our channel is unusually large, we have reexamined this question by doing careful measurements of the steady-state levels. An additional purpose in carrying out these measurements was to allow direct comparison with ion-trapping measurements. These will be discussed elsewhere.

The force density F_{sn} was determined from Eq. (18) by measuring the temperature difference between T_1 and T_4 using the procedures described above. Most measurements were taken with the grid covering the open end of the channel, although the steady-state results were in fact not sensitive to the presence of this addition. Compar-

isons between theory and experiment must be based on Eqs. (16a)–(16c). We first estimate $\bar{L}$ in the traditional way, that is from Eq. (16c) by assuming $I_{\parallel}=\frac{2}{3}$, $I_l=0$, as would be appropriate for an isotropic tangle. $\bar{L}^{1/2}$ plotted against v_{ns} then exhibits the familiar nonzero intercept shown in Fig. 11, which is nowadays recognized[6] as arising from the logarithmic variation of β with $\bar{L}$. The values of $\bar{L}$ so obtained are accurate enough to estimate β from Eq. (2), using the theoretical relationship $\overline{|s''|}=c_1\bar{L}$ derived in Ref. 6. A more careful analysis based on Eq. (16b) can then be carried out by plotting $\beta(F_{sn}/\rho_s\kappa\alpha v_{ns})^{1/2}$ against v_{ns} to determine $(c_L^2 I_{\parallel}-c_L^3 I_l)^{1/2}$. As shown in Fig. 11, this gives the straight line extrapolating through zero predicted by the scaling theory. The values of $(c_L^2 I_{\parallel}-c_L^3 I_l)$ obtained in the present experiments are compared with theory and with values obtained by other workers in Fig. 12.

The homogeneity of the turbulence in the flow direction was also investigated by measuring temperature differences between each pair of resistors along the channel. We find that ∇T appears to be constant along the channel to within a few percent, which is the accuracy of our measurements. This is true whether or not a grid is placed across the open end. Previous experiments[3] have shown that the line-length density is also approximately constant in the spanwise direction, except, possibly, very near the walls. All of these measurements are, of course, done at large line-length densities, where homogeneity is a reasonable expectation. As we will discuss later, the situation may be quite different in the onset regime.

The overall conclusion to be drawn from the steady-state measurements is that F_{sn} measured in our large channel agrees with theory and with other experimental observations to about the same degree as all previous experiments. Although there is some indication in Fig. 12 of a tendency toward lower values of $\bar{L}$ as the channel size increases, there is no evidence for the large deviations claimed by Barenghi *et al.*[13] The degree of homogeneity in the developed limit is quite high so that the transient behavior measured there should, in fact, be characteristic of the homogeneous state.

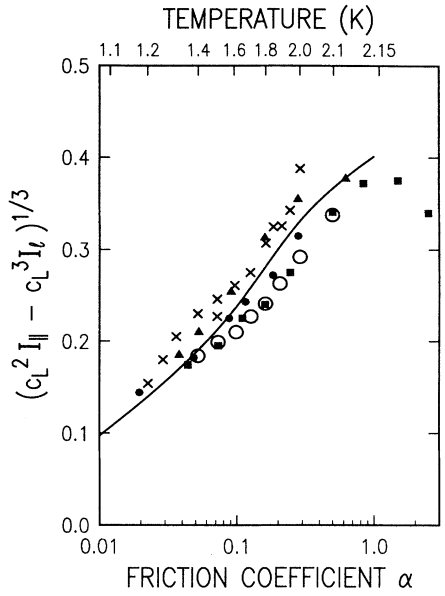

FIG. 12. Comparison of the mutual friction force coefficient measured in our experiment (open circles) with selected previous experiments and with the theory of Ref. 6. Crosses represent pure superflow in a 0.0057 by 0.057 cm channel (Ref. 14), dots represent counterflow in a 0.0366-cm capillary (Ref. 15), triangles are counterflow in a 0.240 by 0.645 cm channel (Ref. 1), and squares represent counterflow in a 1.0 by 1.0 cm channel (Ref. 4). The line is the theoretical prediction.

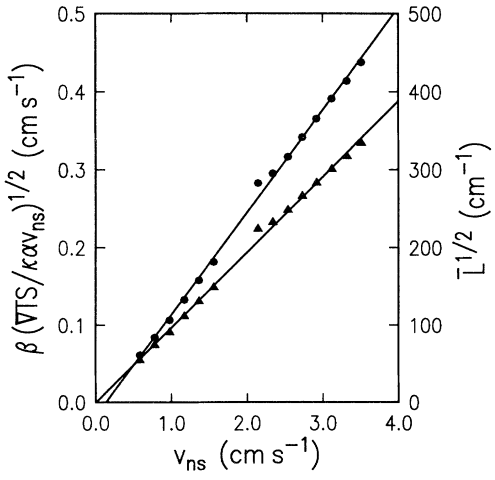

FIG. 11. Steady-state line-length density as a function of relative velocity, measured at 1.6 K. The dots indicate nominal values of $\bar{L}^{1/2}$ derived in the traditional way from Eq. (16c) by assuming $I_{\parallel}=\frac{2}{3}$ and $I_l=0$. Triangles indicate the quantity $\beta(\nabla TS/\kappa\alpha v_{ns})^{1/2}$ which by scaling theory should extrapolate through zero and equal c_{Lm}/v_{ns}. The lines are least-square fits.

B. Small-amplitude transients

As discussed in Sec. II C, small- or moderate-amplitude transients offer the best chance of relating the observed transients to the microscopic theory in a simple way. In particular, for $\bar{L}_f/\bar{L}_i\simeq 1$, all of the transient behavior should be described by Eq. (11) with I_l and c_2^2 taking their steady-state values. True to the dictates of our experiment, we consider the modified density $\bar{L}_m=(I_{\parallel}-c_L I_l)\bar{L}$ as the quantity which can be directly extracted from the signal, assuming homogeneous turbulence and a known value of v_{ns}. From Eqs. (16c) and (18), $\bar{L}_m$ is then just equal to $S\nabla T/\kappa\alpha v_{ns}$. Equation (11) can now be written in the form

$$\frac{d\bar{L}_m}{dt}=\alpha I_{lm}\left[v_{ns}\bar{L}_m^{3/2}-\frac{\beta}{c_{Lm}}\bar{L}_m^2\right], \tag{20}$$

where

$$I_{lm}=I_l/(I_\parallel-c_L)^{1/2} \tag{21}$$

and

$$c_{Lm}=c_L(I_\parallel-c_L I_l)^{1/2} \tag{22}$$

are the modified scaling constants that can be used to fit the data. The latter of these is of course just the quantity already determined from the steady-state measurements and plotted in Fig. 12 as discussed above. Hence, at a given temperature a *single* additional constant I_{lm} should suffice to fit transients at all power levels and of all amplitudes (provided that they are not too large).

Figure 13 and 14 show typical fits of Eq. (20) to a very small transient and a rather large transient, respectively. The spikes arise partly from real switching transients and partly from the fact that the program which extracts $\bar{L}_m$ from F_{sn} assumes that v_{ns} is switched on discontinuously, whereas in reality it is turned on over a period of about 30 ms. The agreement is very sensitive to the value of c_{Lm} and moderately sensitive to I_{lm}, the former typically being determined to 0.5% and the latter to 10%. We find that the entire experimentally accessible range of transients is similarly well modeled by Eq. (20), with values of c_{Lm} that agree well with the steady-state value, and with a *single* value of I_{lm}. It is noteworthy that the same value of I_{lm} fits both the observed growth and decay behavior, and does so for all kinds of transients. We do not see any convincing evidence for the kind of finite-amplitude deviations described in Sec. II C.

Values of I_{lm} are predicted as a function of temperature by the microscopic theory of Ref. 6. Figure 15 compares our experimental determinations against these calculations. The agreement is seen to be quite reasonable,

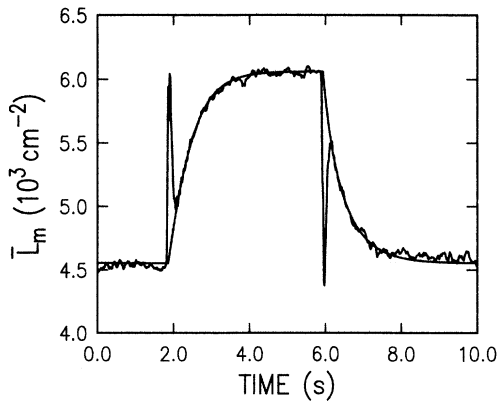

FIG. 13. Fit of Eq. (20) to the transient shown in Fig. 10. The fitting parameters are $c_{Lm}=0.0928$ and $I_{lm}=0.65$.

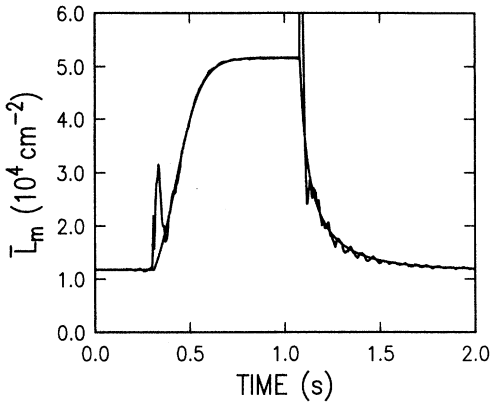

FIG. 14. Fit of Eq. (20) to a much larger transient in which the heater power is switched from 0.0654 to 0.1294 W cm^{-2}, also at $T=1.6$ K. The fitting parameters here are $c_{Lm}=0.0937$ and $I_{lm}=0.65$. The value of c_{Lm} determined from Fig. 11 is 0.096 ± 0.003.

although the measured values of I_{lm} and c_{Lm} indicate a vortex tangle which is somewhat more strongly polarized with respect to the local binormal while at the same time being somewhat more kinky than the theoretical tangle. We conclude that Eq. (11) provides a satisfactory description of all aspects of moderate-amplitude transient behavior, and that the required fitting parameters are satisfactorily predicted by the underlying theory.

It is preferable to use Vinen's equation in the form of Eq. (11), which relates much more directly to the underlying physics of the vortex tangle than Vinen's phenome-

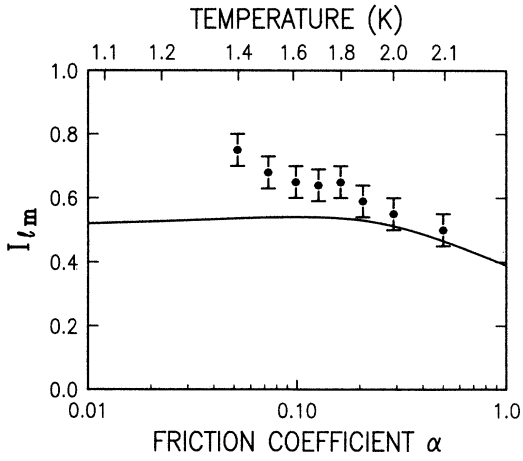

FIG. 15. Values of I_{lm} obtained from fitting the transient response of the vortex tangle to a sudden change in v_{ns}. The line is the theoretical prediction of Ref. 6. The 1.4-K point may be unreliable because of equilibration problems.

nological formulation [Eq. (12)]. The original Vinen parameters χ_1, χ_2 can be extracted from our measurements, but this can only be done approximately because the measurement determines the modified parameters I_{lm} and c_{Lm} defined in Eqs. (21) and (22), rather than I_l and $c_L = I_l / c_2^2$, which appear in Eq. (11). To sufficient accuracy for present purposes, the conversion can be made using the homogeneous-tangle approximation $I_{\parallel} - c_L I_l = \frac{2}{3}$. By studying the growth of the vortex tangle, Vinen deduced a χ_1 roughly constant at 0.29. Noting that $\chi_1 = (\frac{2}{3})^{1/2} I_{lm}$, we see from Fig. 15 that our values are about twice as high as those obtained by him. Once χ_1 has been established, Vinen uses the relation $\chi_1/\chi_2 = 2\pi\alpha\beta/\kappa c_L$ to deduce χ_2 from the steady-state determination of c_L. Primarily because of our higher value of χ_1, but also because our measured values of c_L are somewhat smaller than Vinen's, we extract χ_2's that are about two to three times larger. The origin of these discrepancies is not clear, but they should perhaps serve as a warning against an excessively quantitative application of the Vinen phenomenology, and an indication that there may remain some channel-dependent effects that have not yet been well understood.

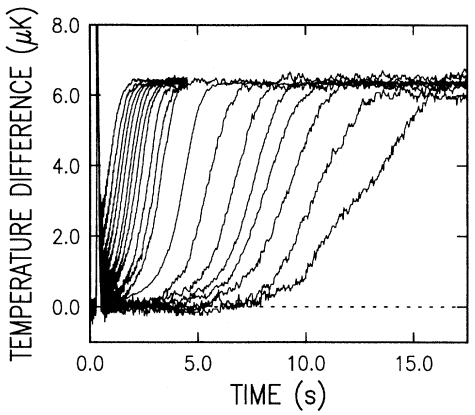

FIG. 16. Typically family of recovery curves generated by switching the heater back on after the vortex tangle has been allowed to decay for various lengths of time. Here the steady-state heat flux density was 0.064 W cm^{-2}, corresponding to $v_{ns} = 1.15$ cm s^{-1} at $T = 1.6$ K, where these curves were taken. The decay times vary from 0.40 to 2700 s.

C. Anomalous decay

In addition to the above method of finding χ_1 and χ_2, Vinen determined χ_2 directly from the free decay of the vortex tangle when the driving velocity is turned off. Using this approach he finds values of χ_2 which are *much lower still,* and this has been confirmed by Milliken *et al.*[5] The results we have presented in the previous section, on the other hand, show no evidence for any such anomalously slow decay, and clearly contradict the idea that the decay of superfluid turbulence is governed by a ratio $I_{lm}/c_{Lm} = c_{2m}^2$ that is much smaller than suggested by the theory. What is the origin of this discrepancy? Previous experiments showing slow decay established a vortex-tangle state at a rather high initial level, then suddenly reduced v_{ns} to zero and monitored the resulting time variation in $\bar{L}$. Since in our experiment the signal is proportional to v_{ns}, we cannot use this direct procedure and must resort to a more indirect "waiting time" method first introduced by Vinen. Suppose Eq. (20) is assumed to describe the growth of the vortex tangle; then the time needed for the tangle to achieve equilibrium when v_{ns} is applied is a strong function of the initial value of $\bar{L}_m$. Thus, the value reached by $\bar{L}_m$ after some decay time t_d can be estimated by reapplying v_{ns} and fitting Eq. (20) to the resulting recovery curve. Any series of such measurements, such as the one reproduced in Fig. 16, does indeed exhibit the expected qualitative behavior.

An interesting feature exhibited by Fig. 16 is that, for the longer wait times, the growth is not accurately described by Eq. (20), becoming considerably more stretched out as t_d increases and $\bar{L}(t_d)$ accordingly decreases. We speculate that the origin of this phenomenon lies in an increasing amount of spatial inhomogeneity in the growth process as it starts from lower and lower levels, leading to a recovery rate which is different in different parts of the channel. We do not find any evidence for such inhomogeneity in the streamwise direction, the recovery curves having the same stretched-out shape when measured between any two thermometers in the channel. Thus, we surmise that the deviations from Eq. (20) which gradually develop as t_d becomes large reflect the fact that the driving velocity v_{ns} becomes more and more nonuniform across the channel at low line-length densities. It is known experimentally[3] that at high turbulence intensities the normal-fluid velocity profile adjusts itself to be practically uniform over the cross section of the channel. It is to be expected, however, that as the line-length density becomes small, the normal-fluid velocity profile will approach the Poiseulle profile of a classical fluid in the absence of mutual friction. There is no satisfactory model which would allow us to calculate the profile and the line-length density self-consistently. Hence, our explanation is offered here only as a reasonable speculation inviting further study.

Fitting Eq. (20) to a series of recovery curves produces a decay curve such as the one shown in Fig. 17. For long decay times, where the experimental recovery curves do not coincide with the theory, the fit is made so that the centers of the curves agree. This introduces uncertainties of up to 30% at very long times, but insignificant errors at the shorter times of primary interest here. The method of plotting used in Fig. 17 is based on the fact that the solution of Eq. (20) for free decay ($v_{ns} = 0$) can be written in the simple form

$$\frac{1}{\beta \bar{L}_m} = \frac{1}{\beta_i \bar{L}_{mi}} + \frac{\alpha I_{lm}}{c_{Lm}} t \ , \tag{23}$$

where the i subscript refers to the initial condition. The slope of the experimental curve in Fig. 17 is about 0.09.

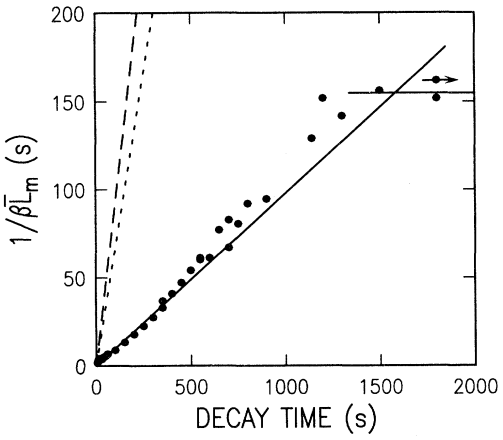

FIG. 17.Vortex-tangle decay curve, obtained at 1.9 K for an initial heat flux density of 0.108 $W\,cm^{-2}$, corresponding to $v_{ns}=0.92\ cm\,s^{-1}$. The point with the arrow was taken after a decay time of 5880 s. The solid lines are drawn to guide the eye. The dashed line is the decay behavior expected on the basis of the direct transient measurements; the dotted line is the behavior predicted by the theory of Ref. 6.

This is to be compared with the value 0.93 obtained by fitting the small-amplitude transients or the value 0.66 predicted by the theory of Ref. 6. The value of I_{lm} one would deduce from Fig. 17 is about 0.06, in approximate agreement with estimates that one can obtain from Ref. 1 and 3. Hence, we too observe the anomalously slow decay. The apparent contradiction is clarified by examining the regime very near $t_d=0$. Figure 18 shows that there

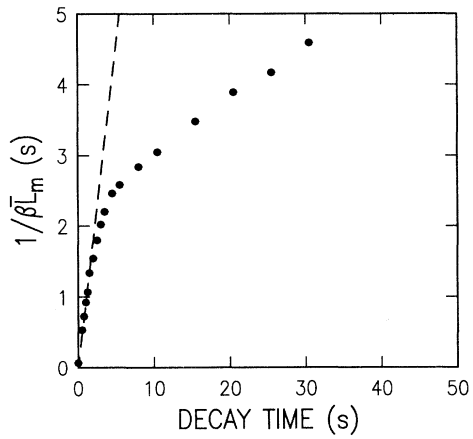

FIG. 18. Blowup of Fig. 17 at short decay times, showing the sharp crossover to the anomalously slow stage of vortex-tangle decay. The dashed line is obtained from fitting the direct transient measurements. The point at zero decay time is the initial steady-state value.

are in fact *two* distinct decay regimes, the vortex tangle switching from the rapid decay characteristic of the homogeneous state to a regime of much slower decline. It is very interesting to note that this rather sharp transition was also observed by Vinen, although his interpretation focused on the slow stage as representing the characteristic behavior of the homogeneous vortex tangle. It is only now clear that it is in fact the initial period of fast decay which is consistent with the well-understood properties of the homogeneous state, while the slow stage must represent something else entirely.

What is a plausible physical explanation for the occurrence of slow decay? During our extensive computational investigations, we have found no indication that this kind of behavior can arise within the context of the vortex-tangle model, as might be possible, for example, if strong internal correlations were to develop within the tangle. Consider, on the other hand, what would happen in an infinitely long (or toroidal) channel if the driving mechanism were turned off and the vortex tangle were allowed to relax *together* with v_n and v_s. The mutual friction is initially large so that v_n and v_s are quickly entrained to almost the same velocity. In the special case of counterflow this velocity is zero, but in general it can be large, the two fluids moving together. In either case one would expect $\bar{L}$ to decrease as predicted by Eq. (20) with v_{ns} set to zero. As this is happening, however, the normal fluid continues to slow down because of its viscous interaction with the channel walls. Since v_s can only slow down by transferring its energy to the normal fluid *via* the mutual friction mechanism, it lags behind in its deceleration and a certain mismatch between v_n and v_s is maintained. This mismatch is capable of sustaining the vortex tangle, but at a much lower level. Consequently, once $\bar{L}$ has decayed down to this level, the system will cross over to a different dynamical regime wherein $\bar{L}$, v_n, and v_s all decay together in a self-consistent fashion. At this stage, the decay of the vortex tangle is controlled, not by vortex-tangle dynamics, but by the normal-fluid viscosity.

Our contention is that our channel experiment reflects a complicated version of this sequence. Although the situation is obviously not well controlled or characterized, it is suggested that the act of switching off the heater does not reduce v_n and v_s everywhere to zero in an instant, but rather leaves behind some kind of large-scale random motion in v_n and v_s. These fields will now relax (together with the vortex tangle) in the manner just described, leading to a crossover from the vortex-tangle decay governed by Eq. (20) to a self-consistently coupled decay limited by the normal-fluid viscosity.

The interpretation offered here may seem somewhat speculative, but it allows one to construct a very simple one-scale model which reproduces many of the features we observe. We assume Eq. (20) to apply, but now interpret v_n and v_s as representing the typical magnitudes of the random fields. The superfluid velocity is affected only by the mutual friction force

$$\rho_s(dv_s/dt)=\rho_s\kappa\alpha\bar{L}_m(v_n-v_s)\ , \tag{24}$$

while the normal fluid is affected both by mutual friction and by viscosity:

$$\rho_n(dv_n/dt) = -\rho_s\kappa\alpha\bar{L}_m(v_n - v_s) - \eta v_n/d^2 \ . \qquad (25)$$

The last term is an estimate for $\eta\nabla^2\mathbf{v}_n$, d representing the typical scale over which v_n varies. It could represent the scale of normal-fluid turbulence or the effect of the viscous boundary in the channel. It is essentially an adjustable parameter, but should bear some reasonable relation to the channel size D in order for the argument to make sense. We now start Eqs. (20), (24), and (25) off from an initial state in which $\bar{L}_m$ is assigned a value corresponding to some initial driving velocity. A large out-of-balance value comparable to this driving velocity is assigned to v_s, while v_n is set equal to zero. In the actual computations we have set the initial value of v_s equal to the rms sum of the driving velocity components v_n and v_s, and we have used $d = D/15$. Our results are not particularly sensitive to these choices, but it does appear to be important to put the out-of-balance motion into the superfluid component. The computation (Fig. 19) then exhibits the predicted entrainment of the two velocities, and gives rise to a well-defined crossover in the vortex-tangle decay. Under certain circumstances the equations give rise to an overshoot effect as seen in Fig. 19. We have not observed this effect, but it is interesting to note that such effects were observed by Vinen.[1] These simple equations are surprisingly successful in modeling the observed behavior. Figure 20a shows data taken by starting from various initial power levels at 1.9 K. It can be seen from Fig. 20b that these measurements are, in fact, semi-quantitatively reproduced. We have also obtained waiting-time decay curves at various temperatures down to 1.4 K. These represent a significant additional test of the model equations, since α varies by a factor of 4 and η/ρ_n by a factor of 6 over this temperature range. As illustrated in Figs. 21(a) and 21(b), the same kind of semi-quantitative agreement is obtained without any additional adjustment of parameters.

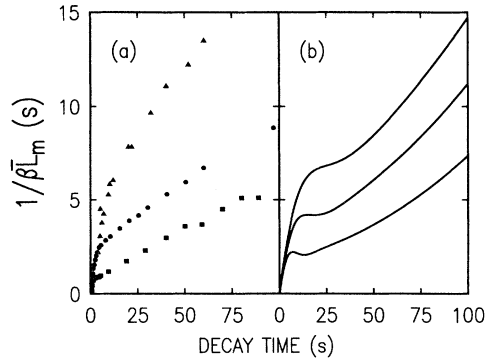

FIG. 20. (a) Modified line-length density vs decay time measured at 1.9 K for three different initial states. The initial heat flux densities are 0.065 W cm^{-2} (triangles), 0.108 W cm^{-2} (circles), and 0.237 W cm^{-2} (squares). (b) Predictions of the coupled equations (20), (24), and (25) for the same conditions, computed as discussed in the text.

Equations (20), (24), and (25) cannot be taken very seriously as a description of what is going on in our channel. It is not clear what the actual flow states are, what the choice of d signifies, or why putting all of the initial motion into the superfluid velocity field gives the best fit to the data. Nevertheless, the qualitative success of these equations in predicting not only two distinct regimes of decay, but also the rates of decay, the location of the crossover point, the dependence of the decay shape on the initial condition, and the variations of the decay curves with temperature supports the correctness of the basic physical idea. We wish to point out that our obser-

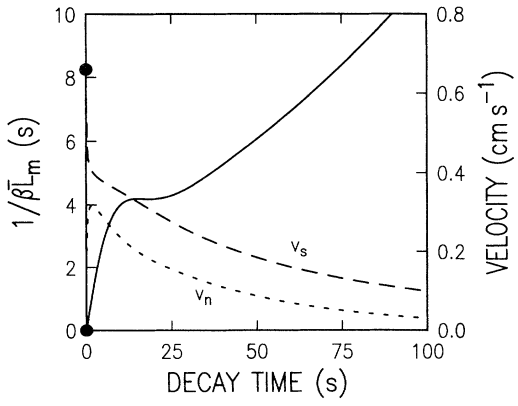

FIG. 19. Model calculation corresponding to the experimental conditions of Figs. 17 and 18. Note how quickly v_n and v_s become substantially entrained. The initial values of v_n and v_s are indicated by dots.

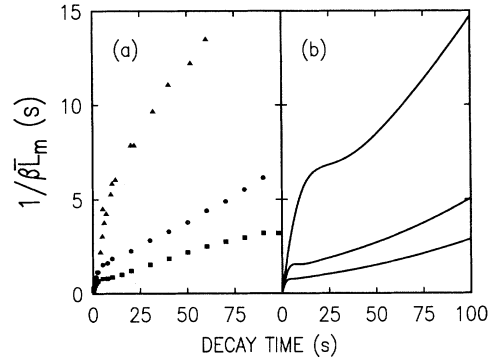

FIG. 21. (a) Modified line-length density vs decay time for various temperatures. The temperatures and initial heat flux densities are 1.9 K and 0.065 W cm^{-2} (triangles), 1.6 K and 0.065 W cm^{-2} (circles), and 1.4 K and 0.043 W cm^{-2} (squares). (b) Predictions of the coupled equations (20), (24), and (25) for the same conditions, computed as discussed in the text.

vations have wider significance than just the resolution of an old puzzle in vortex-tangle dynamics. Suppose the superfluid is made turbulent in the conventional macroscopic sense, that is, by stirring it or by pumping it rapidly through a pipe. Although this kind of turbulence is of considerable interest both from a fundamental and a technological standpoint, very little is known about it. Pressure drop measurements made on high-velocity superfluid transfer through relatively large pipes show classical behavior,[16] and it has been asserted that macroscopic turbulence in superfluid ^{4}He is indistinguishable from classical turbulence. The notion here is that a vortex tangle is present and that the resulting mutual friction couples $\mathbf{v}_s$ and $\mathbf{v}_n$ together so strongly that they move as one fluid. Of course, if these two components of the motion were indeed locked together, there would be no relative motion to sustain the vortex tangle. More fundamentally, $\mathbf{v}_s$ and $\mathbf{v}_n$ obey different equations, and, in particular, $\mathbf{v}_s$ can exhibit macroscopic vorticity only as a consequence of long-range correlations in the vortex-tangle structure. The vortex tangle, however, has its own internal dynamics. Thus, it makes more sense to think in terms of a new dynamical state in which macroscopic random motions in $\mathbf{v}_s$ and $\mathbf{v}_n$ interact strongly through the mutual friction, while at the same time the tangle microstructure is maintained by the mismatch between these two macroscopic components of the motion. For want of a better name, we call this new state *coupled turbulence*. It presumably represents neither classical turbulence nor the simple vortex tangle, but must rather be thought of as a self-consistent, strongly interacting combination of the two. The results we have reported, qualitative as they are, are the first to give a clear indication for the existence of such a state. It is worth pointing out that the coupled-turbulence state produced in channel experiments is apparently rather weak. The method of plotting we have chosen in Figs. 17–19 somewhat obscures the fact that $\bar{L}_m$ has decayed to only a few percent of its original value by the time the crossover occurs. In contrast, it is interesting to note that the ultrasonically generated vortex tangle of Ref. 3 does not show a crossover, but decays anomalously slowly right from its initially high line-length density state. Thus, ultrasonic agitation seems to produce steady-state coupled turbulence directly, and with a much higher intensity than is achieved in our channel. It should prove of considerable interest to study these issues further and to reinterpret previous experiments from our new point of view.

D. Other observations

One of the unanswered questions in superfluid dynamics is how the vortex-tangle state is initiated. Vortex-vortex reconnection allows quantized vortices to multiply, and thus permits the tangle to be initiated from a few remanent vortices which may be there to start with. There is some evidence[17–19] that such vortices are always present, pinned metastably between irregularities on the channel walls, and it has recently been shown[7] how a few such vortices can interact to create and maintain the vortex-tangle state. The relevance of these conceptually satisfying ideas to actual observations, however, remains largely unexplored. In contrast to the fully developed limit, where theory and experiment now seem to agree in every important respect, it is proving more difficult to understand the rather complicated properties of the onset regime. Some key ideas may still be missing, and it is in this spirit that we report the following additional qualitative observations.

First, we note from Fig. 17 that the recovery curves eventually saturate, typically after the vortex tangle has been allowed to decay for more than about 30 min. In other words, the apparent vortex line-length density derived by fitting Eq. (20) to these curves does not decay all the way to zero. It may be of interest to note that the saturation value of $\bar{L}$ obtained in this way is on the order of 10 cm^{-2}, which is on the order of the critical line-length density found by Tough and co-workers.[12] It may also be relevant that it is comparable to the remanent vortex line density estimated by Awschalom and Schwarz,[19] and that the time required to reach it is of the same order of magnitude as they observed. From the theoretical point of view developed in Ref. 7, however, it does not seem that the vortex tangle can develop homogeneously from an initial distribution of pinned vortices. Furthermore, Tough and co-workers do not, in fact, find that $\bar{L}$ saturates at the critical value, but that it drops abruptly to zero there. We suspect therefore that the saturation of $\bar{L}$ we observe represents a low level of ambient vortex turbulence in our Dewar, arising from the effects of heat leaks, the bath regulation heater, and the experimental heaters. Some support for this is provided by the observation that the ambient value of $\bar{L}$ becomes considerably larger as T becomes smaller. If this picture is correct, then a true subcritical state is normally achieved only in smaller channels, where the critical line-length density is much larger than any ambient contamination.

We feel it not unlikely that all large-channel experiments, including those of Vinen[1] and of Donnelly and co-workers,[4,13] are subject to this ambient effect, and that this is the reason why turbulence is always observed to grow homogeneously in such experiments. In contrast, when channels only a factor of 10 smaller are used, the vortex-tangle state is found to develop by means of propagating fronts originating at the channel ends or at special interior points of the channel.[8,9] We have spent considerable effort in trying to observe propagating turbulent fronts, switching on the heater power after the system has been allowed to settle for a very long time. Those efforts have been unsuccessful. Even placing an extra heater just outside the channel inlet such as to generate a large amount of preexisting vorticity there did not give rise to such a front. The sole effect that could be identified in this case was the diffusion of some of this vorticity into the $T3$-$T4$ region, leading to an earlier rise of the turbulence there. We conclude that the propagation of turbulent fronts in large channels such as ours is too slow a process to compete with the growth of the vortex tangle from its ambient level, and that little can be learned about the initiation of the vortex tangle by doing experiments in such a geometry.

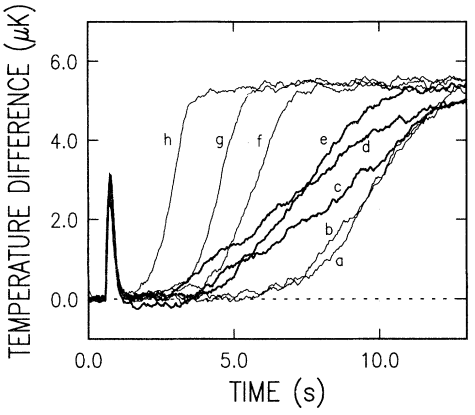

FIG. 22. Growth curves measured between T1 and T4 at $T=1.9$ K. In this case v_{ns} was changed from various very low initial values to a final value of 0.92 cm s^{-1}. The starting values of v_{ns} are (a) 0.00, (b) 0.018, (c) 0.028, (d) 0.037, (e) 0.055, (f) 0.064, (g) 0.074, and (h) 0.106 cm s^{-1}.

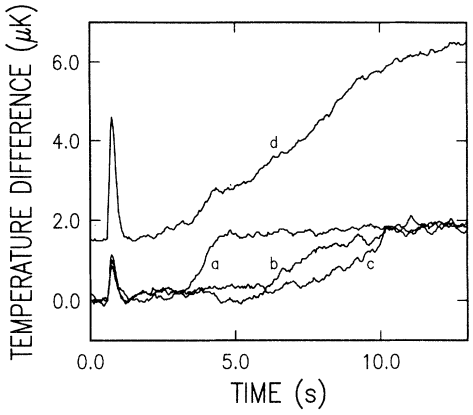

FIG. 23. Growth curves measured in various sections of the channel when the initial v_{ns} is 0.037 cm s^{-1}. (*a*) T1 to T2, (*b*) T3 to T4, and (*c*) T2 to T3. Curve (*d*) is measured between T1 and T4, and has been offset by 1.5 μK. Note that the region near the heater develops first, the region near the inlet some time later, and the region in the center soon after that.

Finally, in attempting to test the ambient-turbulence hypothesis we have noted an interesting effect, which may have some relevance to another peculiar feature of the onset regime—the so-called TI-TII transition. Following its early observation by Brewer and Edwards,[20] extensive studies by Tough and co-workers[21,22] have established that, at least in many situations, vortex turbulence first appears in an atypical, low-level state not well described by vortex-tangle theory. Only at a considerably higher value of v_{ns} does it suddenly switch over into the true vortex-tangle state. There is no explanation for this very unusual phenomenon of an apparently discontinuous transition between distinct turbulent states.

Following earlier authors, we have performed measurements where, instead of letting the turbulence decay down homogeneously before switching the heater back up to its original value, we begin by applying a constant low level of heater power for a long time and then switch the heater up. The idea is to generate a family of curves similar to those in Fig. 16, and by doing the same kind of analysis on the growth curve, to determine the starting steady-state vortex-line density as a function of driving velocity at these very low levels that are not otherwise observable. In attempting this, however, we encounter the unexpected situation shown in Fig. 22. There is now a range of initial conditions, above what we take to be the ambient level, where the growth of $\bar{L}_m$ takes on a very different form from that predicted by Eq. (20). In examining how the growth occurs in various parts of the channel, it becomes obvious that this peculiar behavior is, in fact, due to nonuniformity of the starting steady-state vortex distribution along the channel. Figure 23 can reasonably be interpreted as showing that, in fact, each section grows in accordance with Eq. (20), but that the region near the heater starts out from a state of much higher line-length density. We conclude that, at very low steady-state driving velocities, just above the critical velocity, the line-length density is distributed quite nonuniformly along the channel. Whether this is a consequence of channel end effects (as seems likely) or whether there is an inherent spatial instability in the turbulence is unclear at present, but it leads to the intriguing speculation that the TI state may be a spatially patchy precursor to the homogeneous TII state. In this connection, it is interesting to note that in our experiment the transition to the homogeneous behavior occurs at a v_{ns} of about 0.06 cm s^{-1}. The scaled velocity for the TI-TII transition observed previously in much smaller channels[2] is of order 0.1 cm s^{-1}. This is sufficiently close to be intriguing and suggests that further studies along this line are desirable.

[1]W. F. Vinen, Proc. R. Soc. London, Ser. A **240**, 114 (1957); **240**, 128 (1957); **242**, 493 (1957); **243**, 400 (1957).

[2]See the review by J. T. Tough, in *Progress in Low Temperature Physics,* edited by D. F. Brewer (North-Holland, Amsterdam, 1982), Vol. III, p. 133.

[3]D. D. Awschalom, F. P. Milliken, and K. W. Schwarz, Phys. Rev. Lett. **53**, 1372 (1984).

[4]C. E. Swanson, Ph.D. thesis, University of Oregon, 1985; C. E. Swanson and R. J. Donnelly, J. Low Temp. Phys. **61**, 363 (1985).

[5]F. P. Milliken, K. W. Schwarz, and C. W. Smith, Phys. Rev. Lett. **48**, 1204 (1982).

[6]K. W. Schwarz, Phys. Rev. B **38**, 2398 (1988).

[7]K. W. Schwarz, Phys. Rev. Lett. **64**, 1130 (1990).

[8]V. P. Peshkov and V. K. Tkachenko, Zh. Eksp. Teor. Fiz. **41**, 1427 (1961) [Sov. Phys. JETP **14**, 1019 (1962)].

[9]P. A. Dziwornooh, E. S. R. Gopal, K. Mendelssohn, and S. M. A. Tirmzi, in *Proceedings of the Ninth International Conference on Low Temperature Physics,* edited by J. G. Daunt, D. O. Edwards, F. J. Milford, and M. Yaqub (Plenum, New York, 1965), p. 299.

[10]K. W. Schwarz, Phys. Rev. B **31**, 5782 (1985).

[11]By this we mean an average over a representative selection of instantaneous vortex configurations. As applied to time-dependent phenomena, this average is taken at each moment in time, using solutions evolved from a representative selection of initial conditions.

[12]According to D. R. Ladner and J. T. Tough, Phys. Rev. B **20**, 2690 (1979), the critical line-length density is $\bar{L}_c \cong 6.25/D^2$. Even though this is probably only very approximate, it implies values far too small to be observed directly in our experiment.

[13]C. F. Barenghi, K. Park, and R. J. Donnelly, Phys. Lett. **84A**, 435 (1981); C. F. Barenghi, Ph.D. thesis, University of Oregon, 1985.

[14]L. B. Opatowsky and J. T. Tough, Phys. Rev. B **24**, 5240 (1981).

[15]D. F. Brewer and D. O. Edwards, Philos. Mag. **7**, 721 (1962).

[16]P. L. Walstrom, J. G. Weisend, II, J. R. Maddocks, and S. W. Van Sciver, Cryogenics **28**, 101 (1988).

[17]W. F. Vinen, Proc. R. Soc. London, Ser. A **260**, 218 (1961).

[18]S. C. Whitmore and W. Zimmermann, Jr., Phys. Rev. **166**, 181 (1968).

[19]D. D. Awschalom and K. W. Schwarz, Phys. Rev. Lett. **52**, 49 (1984).

[20]D. F. Brewer and D. O. Edwards, Philos. Mag. **7**, 721 (1962).

[21]K. P. Martin and J. T. Tough, Phys. Rev. B **27**, 2788 (1983).

[22]D. Griswold, C. P. Lorenson, and J. T. Tough, Phys. Rev. B **35**, 3149 (1987).